Dynamical core-hole screening in weak chemisorption systems

N. V. Dobrodey* and L. S. Cederbaum
Theoretische Chemie, Physikalisch-Chemisches Institut, Universität Heidelberg, 69120 Heidelberg, Germany

F. Tarantelli
Dipartimento di Chimica, Università di Perugia, I-06123 Perugia, Italy
(Received 27 June 1997; revised manuscript received 14 October 1997)

Adsorbate core-hole screening in weak chemisorption systems is studied by the example of the $N_2/Ni(100)$ system. Fourth-order Green's-function calculations have been carried out on the N1*s* x-ray photoelectron spectra (XPS) of a linear NiN_2 cluster used as a model of the chemisorption system. Good agreement with the experimental spectra is obtained. A powerful method, based on exact effective Hamiltonians (EEH's) constructed by means of a technique for a unique block diagonalization of Hermitian matrices [J. Phys. A **22**, 2427 (1989)] is used for a detailed analysis of many-electron core-hole states. Two lowest-energy states in the N1*s* XPS of the NiN_2 cluster, split by 1.47 eV (the experimental splitting in the chemisorption system is 1.3 eV), are classified as $\pi \rightarrow \pi^*$ shakedown satellites, whereas two states dominating the region of the so-called ''giant satellite'' are attributed to the main states. The EEH technique allows us to study in detail the dynamical screening of core holes, which is shown to be responsible for the formation of the strong shakedown satellites. A comparative EEH analysis of the core-hole states of the NiN_2 and NiCO clusters explains in simple terms the origin of the very different intensities of the giant satellites observed experimentally in adsorbate spectra of weak and strong chemisorption systems. [S0163-1829(98)07012-X]

I. INTRODUCTION

The ionization of core levels of small molecules adsorbed on *d* metal surfaces is accompanied by strong many-body effects manifesting themselves in intense satellite structures in the x-ray photoelectron spectra (XPS) (see Refs. 1–7 and references therein). It has been observed experimentally that the satellite intensity depends on the strength of the adsorbate-metal interaction. For strong chemisorption [for example, CO/Ni(100)] the satellite region presents a broad feature separated by 5–6 eV from a distinct intense main line. For weak chemisorption [e.g., N_2/Ni(100), CO/Cu(100)] the intensity of the satellite structure is considerably larger than the intensity of the ''main line.'' The core-hole spectra of the respective gas phase molecules consist of a strong main line, taking about 70% of the total spectral intensity, and a wide satellite region separated by an energy gap of ~ 10 eV from the main line. The pronounced difference between the core-hole spectra of adsorbed molecules and those of the gas phase and, especially, the enormously large intensity of the high-energy satellites, which have even been referred to as the ''giant satellites,'' [2–4] attracted wide interest to such adsorbate/metal systems. The core-level XPS of adsorbed molecules have been extensively studied for more than two decades. A large body of experimental results has been collected and a variety of models have been proposed to describe the spectral features of the adsorbate core-hole spectra. A unified notion on the physics of adsorbate ionization, however, is still lacking. Following is an overview of the present state of the problem.

The peculiar feature of adsorbate/metal systems to combine both molecular and solid properties has led to two different lines of attack on the problem: (i) the model Hamiltonian treatment, considering the interaction of discrete adsorbate levels with substrate metal bands; and (ii) the cluster approach, which takes into account only the local adsorbate-metal interaction. The first model focuses on the origin of the giant satellites in the core-hole spectra of adsorbates and has been developed by Schönhammer and Gunnarsson (SG).[8] They used ideas proposed by Lang and Williams, Gumhalter and Newns, and others[9–13] that core-hole screening in adsorbate/metal systems is mainly due to a charge transfer (CT) from occupied substrate metal bands to an initially unoccupied adsorbate level ($2\pi^*$ level in the case of CO and N_2 adsorption), which is pulled below the Fermi level by the attractive core-hole potential. The distribution of the spectral intensity, according to this model, depends on the position of the initially unoccupied adsorbate level in the ionized state and on the degree of hybridization between adsorbate and substrate, i.e., on the strength of adsorption. This model is able to monitor qualitatively the changes of band shapes of the adsorbate core-hole spectra that emerge when going from strongly chemisorbed molecules to cases of weak chemisorption. For the case of the weak adsorbate-metal interaction it has been shown that extra-adsorbate imagelike screening (the screening charge is created at the surface due to the excitation of surface plasmons) becomes dominant.[14,15] This mechanism was widely used for the description of core-hole screening in adsorbates (see Ref. 16) and can be viewed as an alternative to the CT screening (CTS) mechanism: Lovrić, Gumhalter, and Wandelt[17] criticized the SG model applied to the CO/Cu(100) system and, using only the surface plasmon screening mechanism, obtained fairly good agreement with the experimental adsorbate core-hole spectra.

The other branch of models is based on the cluster approach, and one can find several mechanisms of core-hole screening in adsorbates proposed on the basis of cluster cal-

culations: (i) the CTS model where the screening charge is supplied by the metal-π→ligand-π^* excitations accompanying ionization of the adsorbate core level;[18–21] (ii) the model that explains core-hole screening in terms of excitations $\pi_b \rightarrow \pi_a^*$ where the π_b and π_a^* are the bonding and antibonding π orbitals, respectively, unoccupied in the initial state;[22] (iii) the ''cooperative core-hole screening'' mechanism.[23] The limitations of the cluster approach in describing the core-hole screening in adsorbates have not been fully clarified, but the similarity between the spectra of adsorbates and the spectra of corresponding transition-metal compounds[24] provides evidence of a local character of excitations dominating the spectra of adsorbates. This fact justifies to some extent the use of the cluster approach, which accounts for only local properties of adsorbate/metal systems.

The N_2/Ni(100) system is related to the case of weak chemisorption. The N1*s* core hole spectrum reveals a more intense satellite structure compared to the C1*s* and O1*s* XPS of the CO/Ni(100) system, which represents a case of strong chemisorption. This observation is consistent with the predictions of the SG model. According to the model, the ''fully screened'' low-energy peak acquires less intensity from the ''poorly screened'' state (6 eV satellite in the experimental spectrum) due to the weaker adsorbate/metal coupling. The SG model, however, attributes all details of core-hole spectra to the structure of occupied metal bands, which contradicts the experimental finding that the N1*s* XPS of the N_2 molecule adsorbed on different *d* metal surfaces are very similar.[20]

Based on the results of Hartree-Fock (HF) ΔSCF calculations carried out on a linear NiN_2 cluster, it has been concluded that the lowest-energy state is a $\pi \rightarrow \pi^*$ CT screened state and the line at ~6 eV has been attributed to the ''unscreened'' (Koopmans') state.[4] One important detail of the N1*s* spectrum, however, emerged later and was not considered in Ref. 4. It is the splitting (about 1.3 eV) of the lowest-energy line, observed in the angularly resolved N1*s* spectrum of the N_2/Ni(100) system.[25] A most natural way to explain this splitting is to attribute it to the inequivalence of the nitrogen atoms in the N_2 molecule adsorbed vertically on the Ni(100) surface. The author of Ref. 25, however, employing the SG model, concluded that the splitting cannot be attributed to the ionization of the two inequivalent nitrogen atoms. Furthermore, the HF ΔSCF calculations gave a very small splitting of the line due to the inequivalence (0.34 eV).[4] From the results of *ab initio* generalized valence-bond configuration interaction (GVB CI) calculations on the N1*s* spectrum of the NiN_2 cluster it has been concluded that the reason for underestimating the splitting is the neglect of electron correlation in the HF ΔSCF calculations.[20] The splitting obtained in these GVB CI calculations varied between 1.2 eV and 0.9 eV depending on the Ni-N distance and bond energy. According to the calculations, the lowest-energy component of the leading peak in the spectrum is related to the ionization of the outermost nitrogen atom, in accord with the experimental assignment based on the different angular dependence of the intensities of the two components.[6,7,26,27] It should be noted that the HF ΔSCF results of Ref. 4 have been obtained from calculations performed using a $^3\Phi$ ground state (GS) of the NiN_2 cluster and the interatomic distances used were: $R_{\text{Ni-N}}=3.65$ a.u.; $R_{\text{N-N}}=2.074$ a.u. The results of the HF ΔSCF calculations carried out using a $^1\Sigma^+$ GS at $R_{\text{Ni-N}}=3.3$ a.u. and $R_{\text{N-N}}=2.069$ a.u. gave a splitting of 1.6 eV,[28,29] in good agreement with the experimental value.

High-resolution measurements of the N1*s* XPS of the N_2/Ni(100) system have revealed some new satellites that were not detected previously.[27] Using ideas of Refs. 26 and 30 the authors of this experiment have separated spectra of the two inequivalent nitrogen atoms. The spectrum of the outer nitrogen has a richer satellite structure than the inner nitrogen spectrum. A satellite observed at 2.1 eV in the spectrum of the outer nitrogen is absent in the inner nitrogen spectrum. An intense structure at 5.8 eV with a shoulder at 8.5 eV is observed in the outer nitrogen spectrum, whereas only a strong peak at 5.3 eV is observed in the spectrum of the inner atom. The spectral features have been interpreted by the authors of Refs. 7 and 27 using the $Z+1$ model. The lowest-energy lines in the spectra have been assigned to CT screened states ($\pi \rightarrow \pi^*$ CTS). The satellite at 2.1 eV in the outer nitrogen spectrum has been interpreted as a shake-up excitation of the π^* orbital (bonding π_b orbital, which is partially occupied by the CT) to the antibonding lowest unoccupied π_a orbital. The strong satellites around 5–6 eV have been assigned to Rydberg-like transitions of the partially occupied π^* orbital to $3s$-, $3p$-, and $4p$-derived states. The satellite at 8.5 eV has been attributed to the intramolecular $\pi \rightarrow \pi^*$ shake-up transition. A feature at 15 eV has been observed in both of the spectra and also assigned to $\pi \rightarrow \pi^*$ intramolecular excitations.[7] This experimental work has demonstrated that the previous theoretical treatments were not accurate enough to describe the core-hole screening in the N_2/Ni(100) system; none of the above-mentioned theoretical works has predicted these newly resolved satellites in the N1*s* XPS.

Recent *ab initio* restricted CI calculations on the N1*s* XPS of the NiN_2 cluster[28,29] provided a fairly good agreement with the experimental spectra. The authors of Refs. 28 and 29 proposed a new interpretation of the most intense lines in the spectra. According to this, the lowest-energy line in both spectra (the spectra of the inner and outer nitrogens, separated by the authors of Ref. 27) is a $\sigma \rightarrow \sigma^*$ shake-down satellite and the giant satellites are $\sigma \rightarrow \sigma^*$ shake-up satellites that, however, are close to the Koopmans' states.

Obviously, there are numerous and controversial assignments of the satellites in the spectra of the N_2/Ni(100) system. This situation is common for core-hole spectra of adsorbates and sometimes the different interpretations of lines in these spectra are argued to represent rather a semantic issue.[7] We shall show that this problem is only partially a semantic one and propose that the nomenclature used in the field of core-level photoelectron spectroscopy of adsorbates should be revised to bring more clarity into the terms used to assign the spectral features. In the present work we introduce a new method of analysis, which allows one to get a deep insight into the problem of core-hole screening in adsorbates and can also be used for studying other phenomena.

II. THEORETICAL APPROACHES AND METHODS

A. Calculations of core-hole states

The algebraic diagrammatic construction scheme for the one-particle Green's function consistent through fourth order

in the Coulomb interaction [GF ADC(4)] Refs. 31 and 32 has been used to calculate the ionization potentials and intensities of spectral lines. The ionization potentials and intensities appear in the Green's function method in a very natural way: in the spectral representation the Green's function poles are the ionization potentials and the residues at these poles enter the definition of the respective spectral intensities. The configuration space for the GF ADC(4) calculations was generated by allowing all single and double excitations of the two nitrogen core-hole configurations, in the HF orbital basis of the $^1\Sigma^+$ closed shell. The inner metal Ni1s, 2s, and 2p orbitals and their virtual counterpart have been kept frozen. To reduce the dimension of the configuration space all virtual orbitals with energies higher than 55 eV have been frozen too. The final calculation comprises 114 414 configurations. The $^1\Sigma^+$ GS of the NiN_2 cluster have been calculated using the US GAMESS package.[33] The geometry ($R_{\text{Ni-N}}$=3.335 a.u., $R_{\text{N-N}}$=2.069 a.u.) has been optimized by complete active space SCF (CASSCF) calculations using the UK GAMESS package.[34] Four electrons in the highest occupied π orbital and two electrons in the highest occupied σ orbital were correlated by allowing excitations to
the lowest unoccupied two π^* and two σ^* orbitals. It should be noted that electron correlation is very important for a proper description of the NiN_2 cluster bonding properties,[19,35] but the $^1\Sigma^+$ single-determinant HF closed-shell configuration describes the GS rather well. The contracted Gaussian basis set of Roos[36] for Ni, extended by two diffuse p functions[37] and scaled by a factor of 1.5 was used. Furthermore, one diffuse d function[38] was added to the basis set. The nitrogen 9s,5p Gaussian basis set has been contracted to 4s,2p and a polarization d function has been added (α=0.864).[39]

Our present approach conceptually differs from all the previous treatments of the problem in that, by using the ground-state orbital basis, we consider simultaneously the ionization of both inequivalent nitrogen atoms, whereas previously the core ionization was treated as two uncoupled processes localized on each of the two inequivalent atoms. There is clear evidence for the need to consider mixing of configurations having core holes on different nitrogens. The orbitals of the $^1\Sigma^+$ GS of the NiN_2 cluster are markedly delocalized, reflecting to a large extent the symmetry properties of the $1\sigma_g$ and $1\sigma_u$ molecular orbitals of the N_2 molecule. Their energy splitting of $\sim$0.1 eV is also very close to that of the N_2 molecule ($\sim$0.06 eV). Thus at the frozen-orbital level (Koopmans' theorem) the nitrogen core-hole states are largely delocalized. In this respect the NiN_2 cluster essentially differs from other systems where the introduction of even very slight distortions from a highly symmetrical geometry immediately leads to complete symmetry breaking and core orbital localization. The CO_2 molecule, where this effect is brought about by vibronic coupling to the antisymmetric stretching and leads to localization of the O1s core orbitals,[40] is an example of such behavior.

B. Exact effective Hamiltonian method

In the case of core ionization of adsorbates the final ionic states often have a quite complicated structure where many excited configurations are admixed with comparable weights. To acquire additional insight and to describe the physics of ionization in some simple and transparent terms it is useful to replace the interaction of the numerous configurations by the effective interaction of only those that are relevant to the problem. This program can be realized by the technique of block diagonalization of Hermitian matrices. It has been shown in Ref. 41 that a unitary transformation that brings a Hermitian matrix into a block-diagonal form can be uniquely constructed by satisfying the elementary condition that the resulting block-diagonal matrix should be as similar as possible to the original matrix. This condition, which can be viewed as a kind of least action principle, allows one to construct explicitly the required unique transformation.

We begin with the large Hamiltonian matrix $\boldsymbol{H}$, and our goal is to transform it into a block-diagonal matrix $\boldsymbol{\mathcal{H}}$, i.e., to a matrix with blocks $\boldsymbol{\mathcal{H}}_{nn}$ along the diagonal and zero otherwise. Let $\boldsymbol{S}$ be the matrix of eigenvectors of $\boldsymbol{H}$ and $\boldsymbol{\Lambda}$ the corresponding diagonal matrix of eigenvalues. The element blocks of the block-diagonal matrix are then given by[41]

$$\boldsymbol{\mathcal{H}}_{nn}=\boldsymbol{F}_{nn}^{\dagger}\boldsymbol{\Lambda}_{nn}\boldsymbol{F}_{nn}, \tag{1}$$

$$\boldsymbol{F}_{nn}=\boldsymbol{S}_{nn}^{\dagger}(\boldsymbol{S}_{nn}\boldsymbol{S}_{nn}^{\dagger})^{-1/2}, \tag{2}$$

where the $\boldsymbol{S}_{nn}$ are given blocks of the block-diagonal part of $\boldsymbol{S}$:

$$\boldsymbol{S}_{BD}=\begin{pmatrix} \boldsymbol{S}_{11} & \cdots & 0 \\ \vdots & \ddots & \vdots \\ 0 & \cdots & \boldsymbol{S}_{nn} \end{pmatrix}.$$

To clarify the meaning of the block-diagonalization procedure, let us assume that we are interested in the effective interaction of the ith and jth basis configurations in the kth and nth eigenstates of a CI Hamiltonian. To construct the unitary transformation (2) that brings the CI matrix to a block-diagonal form we do not need to know the full eigenvector and eigenvalue matrices of the CI secular problem. It is sufficient to know only the components of the ith and jth basis configurations in the kth and nth eigenstates and the corresponding eigenvalues. In this case the 2×2 exact effective Hamiltonian $\boldsymbol{\mathcal{H}}_{11}$ describing the interaction of the effective configurations originating from i and j is given by Eqs. (1) and (2), where

$$\boldsymbol{\Lambda}_{11}=\begin{pmatrix} \Lambda_{kk} & 0 \\ 0 & \Lambda_{nn} \end{pmatrix},$$

$$\boldsymbol{S}_{11}=\begin{pmatrix} S_{ik} & S_{jk} \\ S_{in} & S_{jn} \end{pmatrix}.$$

Eigenvalues and eigenvectors related to all the remaining configurations are not needed for the construction. The resulting block $\boldsymbol{\mathcal{H}}_{11}$ describes the interaction of effective configurations that are actually the ith and jth basis configurations dressed by the interaction with all the remaining configurations of the CI problem. Of course, this procedure can also be applied when studying the effective interaction of more than two configurations.

There is a useful quantity,

TABLE I. Energies and spectroscopic amplitudes $x_c^{(n)}$ of the N_c1s ionized states of the NiN_2 cluster. A localized representation is used; c refers to the inner and outer nitrogen atoms. Shown are GF ADC(4) results in comparison to the experiment for the N_2/Ni(100)$c(2\times2)$ system. All energies are in eV. The contributions in parentheses denote small admixtures to the ionic states in the order of decreasing importance.

Experiment N_2/Ni(100) (Ref. 27)		GF ADC(4) results				
XPS band	ΔI_n	I_n	ΔI_n	$x_{\text{in}}^{(n)}$	$x_{\text{out}}^{(n)}$	State characterization
1 Main line	0.0	409.00	0.0	−0.013	0.489	$\pi\rightarrow\pi^*+\text{N}1s^{-1}$, $(\sigma\rightarrow\sigma^*)$
2 Main line	1.3	410.47	1.47	0.456	0.014	$\pi\rightarrow\pi^*+\text{N}1s^{-1}$, $(\sigma\rightarrow\sigma^*)$
1 satellite, weak	2.1	411.93	2.93	−0.018	0.103	$\pi\rightarrow\pi^*$
		412.16	3.16	0.130	0.011	$\pi\rightarrow\pi^*$
		413.10	4.10	0.004	−0.006	$\sigma\rightarrow\sigma^*$
		413.83	4.83	0.027	0.0	$\sigma\rightarrow\sigma^*$
2 satellite, strong	5.8	415.48	6.48	−0.628	0.051	$\text{N}1s^{-1}+\pi\rightarrow\pi^*$, $(\sigma\rightarrow\sigma^*)$
3 satellite, strong	6.6	415.90	6.90	−0.048	−0.602	$\text{N}1s^{-1}+\sigma\rightarrow\sigma^*$, $(\pi\rightarrow\pi^*$, N_2 $\pi\rightarrow\pi^*)$
4 satellite, weak	8.5	417.01	8.01	0.117	0.086	$\sigma\rightarrow\sigma^*$, $(\pi\rightarrow\pi^*)$
		417.09	8.09	−0.057	−0.134	$\sigma\rightarrow\sigma^*$, $(\pi\rightarrow\pi^*)$
		418.78	9.78	0.019	0.0	$\sigma\rightarrow\sigma^*$
		419.10	10.10	0.003	0.001	$\sigma\rightarrow\sigma^*$
		419.45	10.45	0.001	−0.002	doubles, $(\sigma\rightarrow\sigma^*)$
		419.66	10.66	0.067	−0.022	$\sigma\rightarrow\sigma^*$
		419.70	10.70	−0.018	−0.057	doubles, $(\sigma\rightarrow\sigma^*)$
		420.17	11.17	0.0	0.017	doubles, $(\sigma\rightarrow\sigma^*)$
		420.27	11.27	0.001	0.089	$\sigma\rightarrow\sigma^*$
		420.28	11.28	−0.016	−0.019	$\pi\rightarrow\pi^*$, $\sigma\rightarrow\sigma^*$
		420.71	11.71	0.047	0.0	$\pi\rightarrow\pi^*$
		420.98	11.98	0.001	0.003	$\pi\rightarrow\pi^*$
		421.23	12.23	−0.001	0.0	doubles, $(\sigma\rightarrow\sigma^*)$
		421.35	12.35	−0.003	−0.022	$\pi\rightarrow\pi^*$
		421.66	12.66	0.015	−0.009	$\sigma\rightarrow\sigma^*$
		421.75	12.75	−0.007	−0.014	$\sigma\rightarrow\sigma^*$
		421.89	12.89	0.020	−0.002	doubles, $\sigma\rightarrow\sigma^*$
		422.01	13.01	−0.002	0.022	doubles, $\sigma\rightarrow\sigma^*$
		422.13	13.13	−0.066	0.021	$\sigma\rightarrow\sigma^*$

$$\boldsymbol{A}_n=(\boldsymbol{S}_{nn}\boldsymbol{S}_{nn}^{\dagger})^{1/2}, \tag{3}$$

which defines the amplitudes of the dressed interacting configurations of the chosen block $\boldsymbol{\mathcal{H}}_{nn}$ of the block diagonal matrix $\boldsymbol{\mathcal{H}}$. These amplitudes show the contributions of the chosen dressed configurations to the eigenstates used for the block diagonalization. The matrices of the exact components of eigenstates $\boldsymbol{S}_{nn}$, the matrix of eigenvectors $\boldsymbol{\mathcal{S}}_{nn}$ of the effective Hamiltonian $\boldsymbol{\mathcal{H}}_{nn}$, and the matrix of amplitudes $\boldsymbol{A}_n$ are related by $\boldsymbol{S}_{nn}=\boldsymbol{A}_n\boldsymbol{\mathcal{S}}_{nn}$.

III. RESULTS

A. Core-level XPS

As already mentioned in Sec. II A, the N1s orbitals of NiN_2 are not localized each on its respective atomic site. Consequently, although electronic relaxation drives towards localization, one cannot *a priori* expect that the final ionic states exhibit fully localized core holes. When calculating the intensities one has, therefore, to take into account possible interference effects arising due to this partial delocalization of the core hole. Although we carry out our *ab initio* GF calculations using the GS orbitals of NiN_2 as input data, it is convenient to transform all quantities to a representation where the N1s orbitals are localized on the inequivalent nitrogen atoms. In this localized representation, which we shall use throughout, the intensity of the nth ionic state in the XPS reads[42]

$$\mathcal{I}_n\sim\left|\sum_c \tau_c x_c^{(n)}\right|^2, \quad c=\text{in,out},$$

where τ_c denote the photoionization amplitudes of the N1s core levels of the inner ($c=$in) and outer ($c=$out) nitrogen atoms in the cluster and $x_c^{(n)}=\langle\Psi_n^{N-1}|\hat{a}_c|\Psi_0^N\rangle$ are the spectroscopic amplitudes of the single hole N_c1s^{-1} states; Ψ_0^N

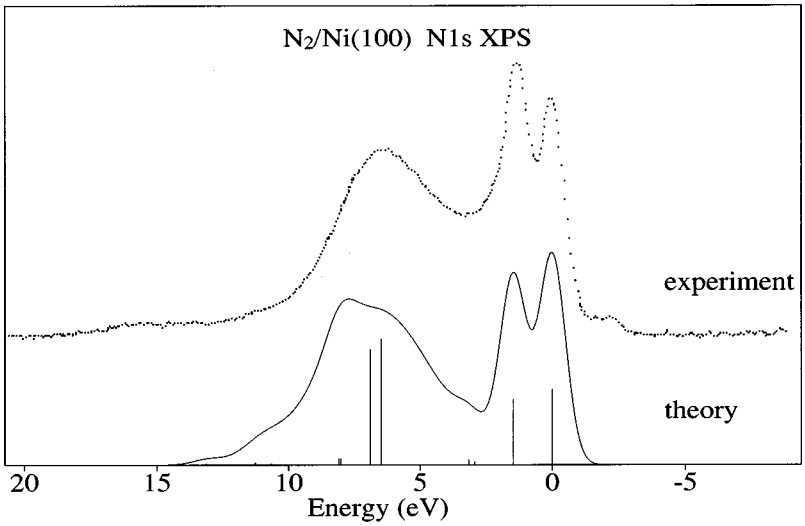

FIG. 1. The computed band shape of the N1s XPS of the NiN_2 cluster in comparison to the experimental N1s spectrum of the N_2/Ni(100)$c(2\times2)$ system (Ref. 27). The vertical lines in the theoretical spectrum represent the energies and intensities of the discrete spectral lines calculated by the GF ADC(4) method.

and Ψ_n^{N-1} denote the GS of the N electron system and the nth state of the ionized $N-1$ electron system, respectively, and the $\hat{a}_c$ is the annihilation operator for the core electron in the cth one-electron orbital.

An analysis of the encountered partial delocalization in NiN_2 and its impact on the intensities in the spectrum will be discussed in detail elsewhere.[43]

The results of the GF ADC(4) calculations on the N1s XPS of the NiN_2 cluster are presented in Table I together with the experimental data of N_2/Ni(100)$c(2\times2)$. Because of the partial delocalization of core holes observed in the N1s-ionized states of the cluster[43] it is not possible to cleanly separate the spectra of the inner and outer nitrogens in the computed spectrum and hence, for the comparison with the experimental spectrum, we combined in Table I the experimental energy positions of the lines in the ''inner nitrogen spectrum'' and ''outer nitrogen spectrum'' [27] to get the whole N1s XPS of the N_2/Ni(100)$c(2\times2)$ system. Correspondingly, we list in Table I the spectroscopic amplitudes $x_c^{(n)}$ of the single hole N_c1s^{-1} states and not the intensities, since the interference due to the partial delocalization is of relevance and requires the knowledge of the photoionization amplitudes τ_c (see above) which will be discussed elsewhere.[43]

The lowest-energy state is mostly localized on the outer nitrogen atom and is separated by the energy interval of 1.47 eV from the next state, which is mainly localized on the inner nitrogen. This assignment is in accord with the previous theoretical treatments[20,28,29] and the experimental assignment.[26,27] Both states are strong mixtures of the N1s single hole configurations and CT $\pi\rightarrow\pi^*$ ones. According to our calculation, these two states are $\pi\rightarrow\pi^*$ *shake-down* satellites (or negative shakeup[44]). It is important to note that, despite the rather large splitting of 1.47 eV, the lowest two states are not completely localized on the inequivalent atoms. A weak but non-negligible delocalization of the core hole is seen for both of the states (Table I). The splitting obtained by the ΔSCF calculation is 1.6 eV.[28,29] The same value was obtained by the CI method.[28,29] The experimental value for the splitting is 1.3 eV.[27] The next two states, which are almost purely $\pi\rightarrow\pi^*$ in character, are considerably delocalized and also are shake-down states. The two shake-down satellites at 4.10 eV and 4.83 eV above the lowest-energy state exhibit a $\sigma\rightarrow\sigma^*$ character. They have very small intensities and cannot be detected experimentally. The states computed at 6.48 eV and 6.90 eV should clearly be assigned to the giant satellite observed in the experimental spectrum at $\sim$6 eV. We classify these two states as the main states (see discussion in next section and Sec. IV) and note that their character is very different. Whereas the state at 6.48 eV is a mixture of the single hole $N1s^{-1}$ and CT $\pi\rightarrow\pi^*$ configurations, with a small contribution of the local metal $\sigma\rightarrow\sigma^*$ excitations, the state at 6.90 eV is a mixture of the $N1s^{-1}$ and these $\sigma\rightarrow\sigma^*$ configurations with a small admixture of the CT $\pi\rightarrow\pi^*$ and intramolecular $\pi\rightarrow\pi^*$ excitations. The $\sigma\rightarrow\sigma^*$ character of the state at 6.90 eV is in accord with a recent CI treatment.[28,29] However, the state at 6.48 eV, which in our results has a dominant CT $\pi\rightarrow\pi^*$ contribution, has also been assigned by this CI treatment to the $\sigma\rightarrow\sigma^*$ local metal shake-up state.[28,29] We relate the two nearly degenerate satellite states at 8.01 eV and 8.09 eV to the experimental feature observed in the spectrum of outer nitrogen at 8.5 eV. These states are almost purely $\sigma\rightarrow\sigma^*$ states and, interestingly, they are well delocalized over the two nitrogen sites.

The experimental ionization potentials for the two lowest-energy states are 399.4 eV and 400.7 eV. To compare the calculated ionization potentials with the experimental values one has to add the work function of $\sim$5.5 eV to the measured ionization potentials, but there is still considerable deviation between the theoretical and experimental values. The main reason for this discrepancy is that we used a small cluster. In the real solid-state situation the interatomic distances can be different from our optimized ones and, what is more important, the number of electrons available for the screening, which lowers the energy, is larger in the real adsorbate/metal system. Two other factors affecting the absolute values of the computed ionization potentials are seen to be less important: we used the core-valence separation approximation[32,45] and did not consider relativistic effects. An estimated relativistic correction to the N1s ionization energy in the atom is $+0.2$.[46] A correction compensating for the effect of the core-valence separation approximation in the N_2 molecule is ~-0.5 eV.[46] These two corrections have opposite signs and almost compensate each other.

The theoretical N1s spectrum of the NiN_2 cluster is shown in Fig. 1 together with the experimental one. The only available high-resolution N1s experimental spectra of the N_2/Ni(100) system are angularly resolved and we used for the comparison to the theoretical spectrum the one measured at the electron emission angle $\theta = 35°$ where the influence of the forward peaking of the ionization amplitude[47] for the inner nitrogen is minimal. To avoid any parameter fitting at this point, we neglected the interference effects arising due to delocalization[43] by calculating the intensities of the spectral lines as the sum of the squared spectroscopic amplitudes of the $N_{in}1s^{-1}$ and $N_{out}1s^{-1}$ configurations (Table I) for the respective ionized states. The band shape of the theoretical spectrum has been obtained by Gaussian broadening of the discrete lines in the spectrum. Different half-widths were used: for all satellite lines the half-width is 0.25 eV and for the two main lines 4.5 eV. In view of the complexity of the system the agreement between the experimental spectrum and theoretical one is very good. We should recall again that we are actually comparing here the theoretical *ab initio* spectrum of a small cluster with the experimental spectrum of a solid-state sample. A question that is of interest in and of itself is why the main-line region and the satellite region of the spectrum of the N_2/Ni(100) system exhibit such markedly different widths. In our view the shake-down satellites are rather a cluster many-body property of the system and hence the width of these cluster states is not strongly affected by solid-state effects whereas the high-binding-energy region is broadened by an amount of the order of the width of the Ni3d band (~ 4 eV).

B. Dynamical screening: NiN_2

It is convenient to make a distinction between statical and dynamical screening. While statical screening is described within the framework of the frozen-orbital approximation of SCF theory[48] and can be viewed as electrostatic screening, dynamical screening is due to many-electron relaxation and correlation effects accompanying ionization.

As seen above, we have characterized the first two lines separated by 1.47 eV in the N1s XPS as $\pi \rightarrow \pi^*$ shake-down satellites and the two lines at 6.48 and 6.90 eV as the main lines, which originate mainly from the single-hole N1s configurations. To clarify the physical origin of these two groups of lines we have performed a detailed analysis of core-hole screening in the NiN_2 cluster. As the first step let us consider statical screening. The creation of a core hole pulls down the energies of occupied and unoccupied orbitals. At the static level of treatment this can lead to a negative shake-up energy if the unoccupied orbital (π^* orbital in the case of NiN_2) is considerably more affected than the occupied one (π). The shake-up energy, i.e., the energy of the satellite configuration $c^{-1}\pi^{-1}\pi^*$ relative to that of the single-hole one c^{-1}, is given by

$$\Delta E^{(c)}_{\pi\rightarrow\pi^*} \approx (\epsilon_{\pi^*} - V_{c\pi^* c\pi^*}) - (\epsilon_{\pi} - V_{c\pi c\pi}) - V_{\pi\pi^*\pi\pi^*}, \tag{4}$$

where ϵ_{π^*} and ϵ_{π} are the energies of the π^* and π orbitals, respectively, V_{ijkl} are the usual Coulomb integrals, and the c denotes the core level. For the sake of simplicity we have omitted in Eq. (4) all the exchange integrals appearing in the full expression.[44] For the ionization of the N1s levels (denoted as 1σ and 2σ) of the NiN_2 cluster we obtained from Eq. (4) the positive shake-up energies: $\Delta E^{(1\sigma)}_{\pi\rightarrow\pi^*} = 6.04$ eV, $\Delta E^{(2\sigma)}_{\pi\rightarrow\pi^*} = 5.16$ eV.

Thus statical screening, although lowering the relative energy of the $c^{-1}\pi^{-1}\pi^*$ CT configuration ($\epsilon_{\pi^*} - \epsilon_{\pi} = 16.11$ eV) and reducing the corresponding $\pi \rightarrow \pi^*$ excitation energy in the neutral NiN_2 ($\epsilon_{\pi^*} - \epsilon_{\pi} - V_{\pi\pi^*\pi\pi^*} = 8.57$ eV), is not alone responsible for the appearance of the negative shake-up (shake-down) satellites in the core-hole spectrum of NiN_2. We must then consider dynamical screening as the main reason for the dramatic lowering of the energy of the $c^{-1}\pi^{-1}\pi^*$ CT configuration relative to the single-hole c^{-1} one, which results in the appearance of intense shake-down satellites. We used the exact effective Hamiltonian (EEH) method described in Sec. II B to study dynamical screening. Here we should mention that although the matrix that is diagonalized in the GF ADC method is not a Hamiltonian matrix, it can be viewed as a CI matrix with modified matrix elements. It is convenient to use for the analysis a localized picture, where the core-hole configurations are described in terms of the N1s atomic orbitals localized on the inner and outer nitrogen atomic sites. The states of interest are those corresponding to the four most intense lines in the N1s core-hole spectrum, i.e., the pair of states at 409.00 eV and 410.47 eV, and the pair of states at 415.48 eV and 415.90 eV. To study the dynamical aspects of core-hole screening we constructed the corresponding 2×2 exact effective Hamiltonians using the computed ionization potentials and spectroscopic amplitudes. As discussed in Sec. II B, no other data are needed for the construction of the EEH. We started from the configuration space comprising two single-hole configurations (the holes in the molecular orbitals representing the N1s levels of the NiN_2 cluster) and all their single excitations (571 configurations). Subsequently, we extended the space step by step by allowing double excitations of occupied orbitals to an increasing number of virtual ones. This procedure enables us to monitor the increase of dynamical screening contributions to the ionic states as a function of the amount of allowed configuration mixing.

The energies of the dressed single-hole and $\pi\rightarrow\pi^*$ CT configurations where the core hole is localized on the inner and outer nitrogen atoms are presented in Fig. 2 as a function of the number of configurations used in the computation. These energies are given by the diagonal elements of the EEH's constructed in the localized basis, using Eqs. (1) and (2). One can see a very strong relaxation of the dressed $\pi \rightarrow \pi^*$ CT configurations at large configuration spaces, and a rather modest relaxation of the dressed single-hole configurations. The c_{in}^{-1} and c_{out}^{-1} dressed single-hole configurations remain the lowest-energy ones up to a dimension of the configuration space of about 22 000. Subsequently, the energy of the dressed $c_{out}^{-1}\pi\rightarrow\pi^*$ charge-transfer configuration quickly drops down and becomes the lowest one at a dimension of the configuration space of about 36 000. At this point, the dressed $c_{in}^{-1}\pi\rightarrow\pi^*$ CT configuration is still the highest-energy one, but it goes further down considerably when approaching a dimension of 60 000. Here, the additional relaxation of the dressed c_{in}^{-1}, c_{out}^{-1}, and $c_{out}^{-1}\pi\rightarrow\pi^*$

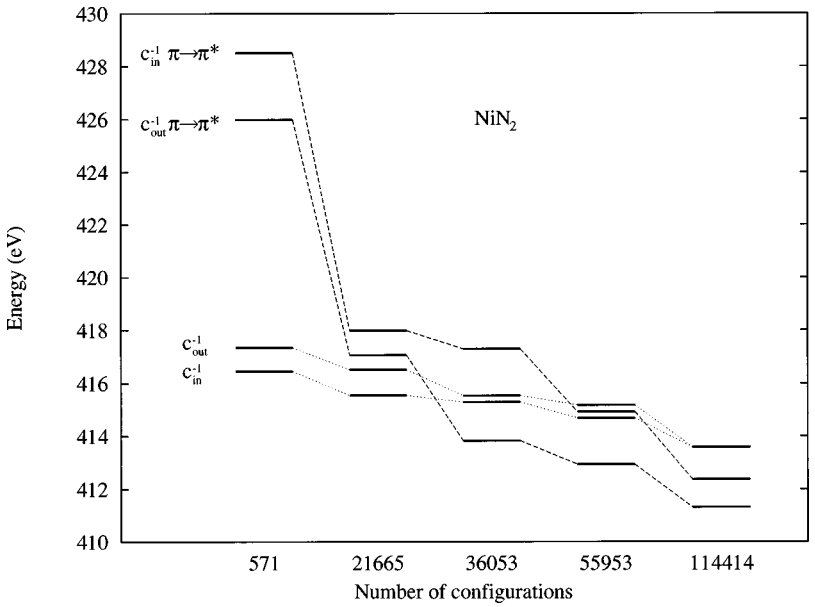

FIG. 2. The energies of the dressed $c^{-1}_{\mathrm{in,out}}$ single-hole and $c^{-1}_{\mathrm{in,out}}\pi\rightarrow\pi^*$ CT configurations as a function of the number of the basis configurations used in the GF ADC(4) calculations of the N1s-ionized states of the NiN_2 cluster.

configurations is seen to be relatively small. Further extension of the space up to 114 000 configurations leads to further energy lowering, in particular, of the dressed $c_{\mathrm{in}}^{-1}\pi\rightarrow\pi^*$ CT configuration. The final result is that the dressed charge-transfer configurations are the lowest in energy. The dressed single-hole c_{in}^{-1} and c_{out}^{-1} configurations are nearly degenerate and situated well above the CT ones. This finding clearly shows that the lowest-energy lines in the core-hole spectrum of the NiN_2 cluster are $\pi\rightarrow\pi^*$ shake-down satellites, whereas the two intense lines dominating the region of the giant satellite should be viewed as the main lines. These two intense lines also have the largest spectroscopic amplitudes $x^{(n)}$ (see Table I), which implies that the weight of the single-hole configuration in the corresponding final states is the largest of all states (see discussion in Sec. IV).

An interesting feature of the computed EEH's should be stressed: while the *energies* of the dressed configurations change considerably, the *interaction* between the dressed single-hole and $\pi\rightarrow\pi^*$ CT configurations is nearly constant for all the dimensions of the configuration space used, and is about 2.3 eV and 3.3 eV for the inner and outer nitrogens, respectively. For all effective Hamiltonians used in the analysis of dynamical screening, the matrices $\boldsymbol{A}$ of amplitudes of dressed configurations [Eq. (3)] are nearly diagonal. This implies that the components of the exact eigenvectors can be obtained just by scaling the respective components of the effective Hamiltonian eigenvectors. The only relevant quantity for the calculation of the spectral intensities in our case is the first diagonal element of the matrix of amplitudes. This value varies slightly from 0.86 to 0.77 when going from the minimal dimension of the configuration space (571 configurations) to the maximal one (114 414 configurations). This rather large value, which is simply the scaling factor mentioned above, shows that the dressed single-hole and $\pi\rightarrow\pi^*$ CT configurations are indeed the relevant ones for the description of core-hole screening in our case. The fact that the matrix of amplitudes is nearly diagonal indicates that the single-hole and $\pi\rightarrow\pi^*$ CT configurations mostly couple to different classes of excitations.

Let us briefly summarize the response of the core-hole configurations in NiN_2 to a hypothetical continuous switching on of the strength of the many-body effects. Both the $\pi\rightarrow\pi^*$ CT satellite and single-hole configurations relax, but the relaxation of the CT configurations is much stronger due to stronger coupling to higher excitations (dynamical screening). The satellite state acquires intensity, borrowing it from the single-hole state essentially through the above-mentioned nearly constant interaction between the two dressed configurations. At some strength of the dynamical screening the energy of the satellite state becomes lower than that of the main state and the intensity acquired by the satellite from the main line becomes considerable. Eventually, we have low-lying intense shake-down satellites in the spectrum and the main lines are situated at higher binding energies. The relaxation of the dressed $c_{\mathrm{in}}^{-1}\pi\rightarrow\pi^*$ CT configuration differs from that of the $c_{\mathrm{out}}^{-1}\pi\rightarrow\pi^*$ one in that it is energetically lowered more efficiently at higher dimensions of the configuration space. This behavior can be explained by the fact that the π^* screening orbital is more localized on the outer nitrogen atom.

C. Dynamical screening in weak and strong chemisorption systems

What is the basic difference between weak and strong chemisorption systems, which is responsible for the different band shapes observed in the experimental XPS? This question is a key point in the problem of core-hole screening in adsorbates. To get an idea of the peculiar feature that makes the core-hole spectra of weak and strong chemisorption systems so different we also performed the analogous EEH analysis of the C1s core-hole states of a linear NiCO cluster, representing the case of the strong chemisorption CO/Ni(100) system. Similarly to the case of NiN_2, we constructed the EEH's using two eigenstates calculated by the GF ADC(4) method, increasing the dimension of the configuration space step by step, and considering two dressed configurations: $\mathrm{C1}s^{-1}$ and $\mathrm{C1}s^{-1}\pi\rightarrow\pi^*$. The energies of these dressed configurations versus the dimension of the configuration space are shown in Fig. 3. Unlike the case of NiN_2

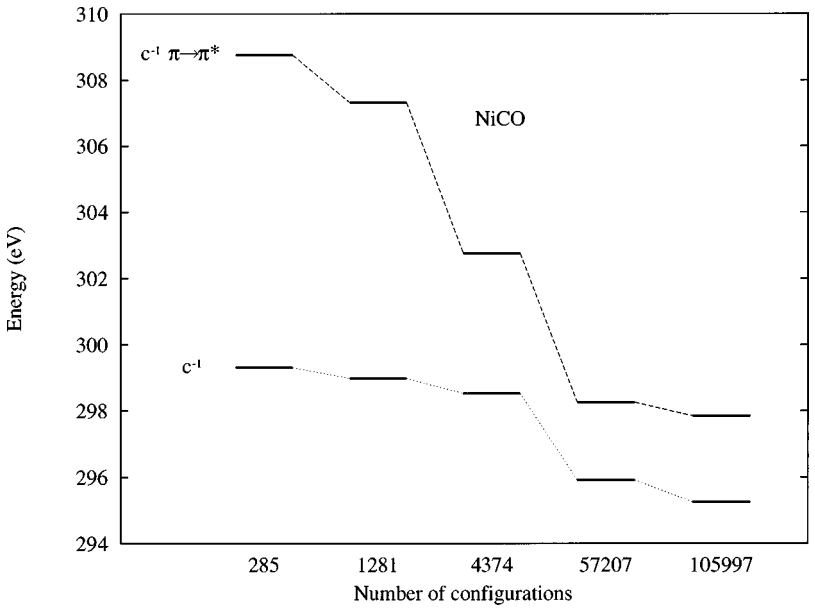

FIG. 3. The energies of the dressed c^{-1} single-hole and $c^{-1}\pi\rightarrow\pi^*$ CT configurations as a function of the number of the basis configurations used in the GF ADC(4) calculations of the C1s-ionized states of the NiCO cluster.

there is no crossover of the dressed single-hole and $\pi\rightarrow\pi^*$ CT configurations. Thus, the lowest-energy state in the C1s XPS of NiCO is the *main-line* state and the most intense satellite (''giant satellite'') is a $\pi\rightarrow\pi^*$ *shake-up* satellite. One can see that the relaxation of the dressed single-hole configuration of NiCO, when enlarging the configuration space, is slightly larger than in the case of NiN_2. However, the relaxation of the dressed $\pi\rightarrow\pi^*$ CT configurations is much stronger in NiN_2 than in NiCO. This different relaxation pattern of core-hole configurations for NiN_2 and NiCO can be explained in terms of the different strength of N_2-Ni and CO-Ni bonding. The CO molecule is more strongly bound to the Ni atom than the N_2 molecule and, consequently, according to the commonly accepted picture of chemical bonding in 3d metal carbonyls,[49] the strength of the $d\pi\rightarrow\pi^*$ backdonation is larger in NiCO than in NiN_2. This means that the number of $d\pi$ electrons effectively available for core-hole screening is smaller in the case of NiCO. Furthermore, a considerable $\pi\rightarrow\pi^*$ charge transfer from Ni to CO is already present in the ground state of NiCO and, therefore, the C1s^{-1} single-hole configuration *a priori* possesses some CT character when compared to the case of NiN_2. This results in a smaller difference between the overall coupling of the single-hole and $\pi\rightarrow\pi^*$ CT configurations to higher excited configurations in the case of NiCO than in that of NiN_2.

We thus arrive at the following picture: both the main and $\pi\rightarrow\pi^*$ CT satellite configurations relax due to strong dynamical screening, but in weak chemisorption systems the relaxation of the satellite configuration relative to the main configuration is larger than in strong chemisorption systems because of the weaker $\pi\rightarrow\pi^*$ charge transfer between substrate and adsorbate in the GS. The relaxation of the satellite configuration in a weak chemisorption case is strong enough to make the corresponding state the lowest-energy state, giving rise to the appearance of shake-down satellites in the core-hole spectra. In cases of strong chemisorption the relaxation of the satellite configuration is less efficient and the main state remains the lowest-energy one in the spectrum. The origin of the lowest-binding-energy state and the state dominating the region of the giant satellite is thus very different for the cases of weak and strong chemisorption: for strong chemisorption the lowest-energy line in the core-hole spectrum is the main line, originating mainly from the single-hole configuration, whereas the giant satellite region is dominated by a conventional $\pi\rightarrow\pi^*$ CT shake-up satellite; for weak chemisorption the lowest-energy line in the spectrum is a $\pi\rightarrow\pi^*$ CT shake-down satellite, whereas the giant satellite should be viewed as the main state.

The EEH technique allows us to go deeper into the details of core-hole screening in adsorbates. In particular, we may also clarify the role of local metal $\sigma\rightarrow\sigma^*$ excitations, which have been suggested[23,28,29,50,51] to be relevant for the screening of core holes in chemisorbed systems. To this end, we extend our analysis to include the leading $\sigma\rightarrow\sigma^*$ configurations explicitly. For NiCO the exact effective Hamiltonian that describes the interaction of the C1s single hole, the $\pi\rightarrow\pi^*$ CT and the $\sigma\rightarrow\sigma^*$ configurations dressed by the interaction with all other configurations reads in eV (only the upper part of the symmetric matrix is shown):

$$\begin{pmatrix} c^{-1} & c^{-1}\pi\rightarrow\pi^* & c^{-1}\sigma\rightarrow\sigma^* \\ 295.36 & -5.34 & -0.63 \\ & 297.82 & -0.68 \\ & & 300.63 \end{pmatrix}$$

To construct this Hamiltonian we used the results of our GF ADC(4) calculation (dimension of the configuration space of 105 997). One can see that the energy of the $c^{-1}\sigma\rightarrow\sigma^*$ dressed configuration is larger than that of the $c^{-1}\pi\rightarrow\pi^*$ one by 2.8 eV. In particular, the interaction between the $c^{-1}\sigma\rightarrow\sigma^*$ and the c^{-1} single-hole dressed configurations is considerably weaker than that between the latter and the $c^{-1}\pi\rightarrow\pi^*$ one. Clearly, the $\sigma\rightarrow\sigma^*$ local metal excitations are of lesser importance and the $\pi\rightarrow\pi^*$ excitations are mostly responsible for the core-hole screening in

the NiCO case of strong chemisorption.

The analoguous analysis has also been performed for NiN_2. Here, we included explicitly in a single EEH the configurations relevant to both the outer and inner nitrogen levels. The EEH has been constructed using GF results (dimension of configuration space: 114 414) and reads as follows:

$$\begin{array}{c} \begin{array}{cccccc} c_{in}^{-1} & c_{out}^{-1} & c_{in}^{-1}\pi\rightarrow\pi^* & c_{out}^{-1}\pi\rightarrow\pi^* & c_{in}^{-1}\sigma\rightarrow\sigma^* & c_{out}^{-1}\sigma\rightarrow\sigma^* \end{array} \\ \begin{pmatrix} 413.74 & 0.047 & -2.18 & -0.014 & 1.105 & -0.018 \\ - & 413.58 & 0.036 & -3.19 & 0.037 & 0.868 \\ - & - & 412.74 & 0.053 & 1.410 & -0.023 \\ - & - & - & 412.07 & 0.064 & 1.847 \\ - & - & - & - & 416.49 & 0.028 \\ - & - & - & - & - & 416.33 \end{pmatrix} \end{array}$$

The $c_{\rm in}^{-1}\pi\rightarrow\pi^*$ and $c_{\rm out}^{-1}\pi\rightarrow\pi^*$ dressed configurations have the lowest energies, whereas the $c_{\rm in}^{-1}\sigma\rightarrow\sigma^*$ and $c_{\rm out}^{-1}\sigma\rightarrow\sigma^*$ have the highest energies among all the dressed configurations considered here. Thus, even considering explicitly the effective interaction with the $\sigma\rightarrow\sigma^*$ transition, the lowest-energy lines in the N1*s* spectrum of NiN_2 are $\pi\rightarrow\pi^*$ CT shake-down satellites. We note that the interaction of the dressed $\sigma\rightarrow\sigma^*$ configurations with the single-hole and $\pi\rightarrow\pi^*$ CT ones is stronger in NiN_2 than in NiCO. This is in accord with the observed admixtures of $\sigma\rightarrow\sigma^*$ excitations to the ionic states of NiN_2 (see Table I).

IV. DISCUSSION

Let us begin our discussion from a seemingly technical aspect, which is, however, very important in our view. There is a widely used practice in the field of theoretical spectroscopy of core levels to use relaxed ionic SCF orbitals for the calculation of core-hole states, in particular, as a basis for CI calculations. It has been shown in numerous examples that the core-hole spectra obtained by CI calculations performed in the basis of SCF orbitals of the neutral GS can be achieved with a significantly smaller dimension of the configuration space when the relaxed ionic basis is used. Of course, the reason for this is that the relaxed orbital basis already incorporates the static core-hole relaxation. In this respect, choosing the relaxed orbital basis is computationally more efficient, although the choice of basis becomes an increasingly marginal issue for large-scale accurate calculations. On the other hand, it is very relevant to realize that the all-important question of interpretation, i.e., of identifying and understanding the physical mechanisms responsible for particular features of the spectra, cannot be adequately tackled in the framework provided by the relaxed orbital basis. To understand in depth the physics of core ionization one has to know the change in the wave functions occurring upon ionization. And the only way to perform such an analysis of ionized states is to compare them with the wave function of the GS of the neutral system. Using the relaxed ionic basis impedes any straightforward comparison of the GS wave function with an ionized state, because the basis sets are different. The relaxed SCF one-particle wave functions of the core-hole state can be very different from that of the GS of the neutral system and one can formally represent the change of the SCF orbitals in the ionized state in terms of excitations of the GS frozen-orbital wave function with a core hole. Therefore, in practice, one has some excited state as a reference for the CI calculation when using the relaxed ionic basis. Evidently, it is impossible to describe exactly this reference excited state in terms of the excitations of the GS one-particle levels to bridge this relaxed ionic basis description to the GS one. Consequently, an interpretation of the results on core-hole states obtained using the relaxed ionic basis can easily be implausible.

The disadvantages of treatments that use the relaxed ionic basis are especially clearly seen when considering the ionization of several core levels in one spectrum. In such cases one usually has a specific basis for each core level, which makes even more problematic a comparative study of the ionization of different core levels. The only basis for many-body calculations on core-hole spectra which affords an immediate and transparent interpretation of the results and allows the disclosure of the core-hole screening mechanism is the GS unrelaxed basis.

Let us now discuss the physics of core-hole screening in adsorbates. A strong charge transfer, which screens the core hole created in the adsorbate, usually leads to intense shake-up satellites in the core-hole spectrum. Under some conditions, the energy of a shake-up satellite relative to the main line can be negative. In this case the *negative shake-up* or *shake-down* satellite appears in the spectrum as the first, lowest-energy, line. What are the conditions to be fulfilled in order to observe negative shake-up energies? It is generally agreed that a main factor responsible for this phenomenon is the electrostatic interaction of the core hole with the electron excited to the vacant screening level. One example where the appearance of a shake-down satellite can be described already at first order in the Coulomb interaction [Eq. (4)] or, in other words, in terms of the electrostatic interaction between electrons and the core hole, is the N1*s* XPS of solid paranitroanilin.[44] In this case the main mechanism responsible for the appearance of the shake-down satellite is the *statical screening* of the core hole. In the case of the N1*s* core-hole spectrum of NiN_2 we see that, although statical screening is important for the energy lowering of the $\pi\rightarrow\pi^*$ CT configurations, it is not sufficient for the appearance of shake-down satellites in the spectrum. The mechanism forming the shake-down satellites is here essentially the

dynamical screening of the core hole.

Idealizing the picture we can classify shake-down satellites by the contributions of statical and dynamical core-hole screening to the energy lowering of the satellite configuration: (i) the *statical shake down*, where statical screening is strong enough for the satellite formation; (ii) the *dynamical shake down*, where the the satellite appears in the spectrum almost entirely due to dynamical screening; (iii) an *intermediate* shake down, where only a combination of statical and dynamical screening can result in the appearance of the shake-down satellite. One can approximately estimate the contributions of statical and dynamical screening in the relaxation of the satellite configuration for the case of NiN_2. The first-order $\pi \rightarrow \pi^*$ excitation energy of the *neutral* system is $\Delta E = \epsilon_{\pi^*} - \epsilon_{\pi} - V_{\pi\pi^*\pi\pi^*} = 8.57$ eV. The statical screening decreases this ΔE by 3.4 eV (see Sec. III B). Dynamical screening further lowers the energy of the satellite configuration relative to the main line by 10 and 12 eV for the state where the N1*s* core hole is mainly localized on the inner and outer nitrogen atoms, respectively. Obviously, dynamical screening dominates the relaxation and we can relate the shake-down satellites in the N1*s* XPS of NiN_2 [and, correspondingly, in the spectrum of the N_2/Ni(100)$c(2\times2)$ system] to case (ii) above.

It is usual to ''automatically'' name the lowest-energy line in the core-hole spectra main line, and refer to structures at higher binding energies as satellites. Sometimes this nomenclature, especially in the case of core-hole spectra of adsorbates, can be misleading and get in the way of the correct physical understanding. Indeed, we believe we have here demonstrated that the only physically meaningful interpretation of the theoretical results for the two lowest energy lines in the N1*s* XPS of N_2/Ni(100)$c(2\times2)$ is that they are shake-down satellites. The main line in a core-hole spectrum should correspond by definition to the ionized state, which is dominated by the contribution of the single-hole configuration. Satellite states ''borrow'' intensity from the main line through many-body effects. We argue that the nomenclature adopted in the field of core-level spectroscopy should adhere as much as possible to this physical content, assigning as main line the most intense line in the spectrum (high-energy photon, i.e., sudden limit), and as satellites the structures having lower intensity.

The comparison of the NiN_2 and NiCO clusters, discussed in the present work, helps us to understand the impact of weak and strong chemisorption on the different core-hole spectral band shapes observed experimentally. The weak and strong chemisorption cases differ by the strength of the $\pi \rightarrow \pi^*$ backdonation, which is a charge transfer in character and, according to the commonly accepted picture of chemical bonding in such *d*-metal systems,[49] is one of the channels of chemical bonding. The stronger the strength of chemisorption, the stronger is the $\pi \rightarrow \pi^*$ CT in the ground state and, consequently, the less charge transfer can occur upon adsorbate ionization to screen the core hole. In the GS of strong chemisorption systems the $\pi \rightarrow \pi^*$ CT is more pronounced and this makes the core-ionized single hole and $\pi \rightarrow \pi^*$ CT configurations more ''similar'' to each other in their interaction with higher excitations. The result is a more similar extent of relaxation of these two configurations due to dynamical screening than is observed in weakly chemisorbed species. Because of this, the energy crossover of the configurations demonstrated for NiN_2 does not occur and one observes a conventional shake-up $\pi \rightarrow \pi^*$ satellite in the core-hole spectrum. Thus, the lowest-energy line in the spectrum corresponds to the main (single-hole) state. In the case of weak chemisorption, the relaxation of the $\pi \rightarrow \pi^*$ CT configuration relative to the single-hole one is more pronounced than that of the strong chemisorption case and this results in the appearance of a shake-down satellite in the spectrum.

The EEH technique provides the ability to extract the energies of dressed configurations and the matrix element of the interaction between them directly from experimental core-hole spectra. For the case of two dressed configurations being considered, assuming that the matrix of amplitudes [Eq. (3)] is diagonal (see Sec. III B), one can easily obtain the energies ϵ_1, ϵ_2 and the interaction matrix element U of the effective Hamiltonian:

$$\epsilon_{1,2} = \tfrac{1}{2}\left(I_1 + I_2 \mp (I_1 - I_2)\,\frac{(1-\xi)}{(1+\xi)} \right);$$

$$U = \frac{\xi^{1/2}}{1+\xi}(I_1 - I_2),$$

where I_1 and I_2 are the energies of the two lines in the spectrum and $\xi = \mathcal{I}_2/\mathcal{I}_1$ is the ratio of their intensities $\mathcal{I}_2$ and $\mathcal{I}_1$.

V. CONCLUSIONS

The GF ADC(4) calculations on the N1*s* XPS of the linear NiN_2 cluster have demonstrated that this small cluster model suffices to reproduce the main features of the experimental N1*s* spectrum of the N_2/Ni(100)$c(2\times2)$ weak chemisorption system. A good agreement between the computed spectrum of the cluster and experimental spectrum is obtained, and this justifies our generalization of the physical picture of core-hole screening obtained for the cluster also to real solid-state systems.

A keystone of our investigation of core-hole screening is the exact effective Hamiltonian technique, introduced in the present paper for the analysis of many-electron core-hole states. The EEH technique provides the description of the core ionization in terms of dressed interacting configurations. This tool allows us to extract from the results of sophisticated many-body calculations a very transparent physics, since one can consider only the configurations that are relevant to the problem, ''dressing'' them by the interaction with all remaining configurations.

The two lowest-energy lines in the N1*s* XPS of the N_2/Ni(100)$c(2\times2)$ system have been definitely assigned by means of the EEH technique to $\pi \rightarrow \pi^*$ shake-down satellites, whereas the two intense lines dominating the region of the giant satellite have been attributed to the main states. The main physical process responsible for the appearance of the strong shake-down satellites in the N1*s* spectrum of the N_2/Ni(100) system is the dynamical screening that dramatically lowers the energy of the $c^{-1}\pi \rightarrow \pi^*$ charge-transfer dressed configuration relative to that of the dressed c^{-1} single-hole one. Shake-down satellites were traditionally considered to appear in core-level spectra due to statical

screening or, in other words, due to the electrostatic interaction of the core hole with valence electrons. The example of the N_2/Ni(100) system shows that in some cases, the statical screening itself is not strong enough to give rise to the appearance of shake-down satellites. An efficient dynamical screening mechanism of the formation of shake-down satellites is disclosed and discussed in detail.

A comparative study of the C1*s* XPS of the NiCO cluster and N1*s* spectrum of the NiN_2 cluster, accompanied by the EEH analysis, has revealed a basic difference between core-hole spectra of strong and weak chemisorption systems: the lowest-energy lines in the spectra of weak chemisorption systems are shake-down satellites and the intense structures in the region of the giant satellite are dominated by main states (the states that mainly originate from single-hole configurations); in contrast to that, the lowest-energy lines in the spectra of strong chemisorption systems are main states, whereas the giant satellites are mainly formed by conventional shake-up excitations. According to our results, adsorbate core-hole screening is stronger in the N_2/Ni weak chemisorption system than in the CO/Ni strong chemisorption system. This can be explained by different strengths of the adsorbate-metal interaction for these two cases. In the case of CO/Ni, the adsorbate-metal interaction is stronger than that of N_2/Ni, leading to a stronger $\pi \rightarrow \pi^*$ charge transfer in the ground state of the CO/Ni system. Therefore, the screening of core holes in ionized states of the CO/Ni system is not as efficient as it is in the N_2/Ni case. The effective number of *d* electrons available for the screening is smaller in the former case due to the stronger charge transfer in the GS. As a result, the single-hole dominated state remains the lowest-energy one in cases of strong chemisorption.

One of the advantages of the EEH technique is that under plausible assumptions one can get effective Hamiltonians directly from experimental data. The effective Hamiltonians, obtained in a systematic way from the experiments on different systems, can be very useful for further understanding the mechanisms of core-hole screening in adsorbates.

We have observed a partial delocalization of core holes for the N1*s* ionized states of the NiN_2 cluster which is an interesting phenomenon that has never been reported before. The discussion of this phenomenon is the subject of a forthcoming paper.[43]

ACKNOWLEDGMENTS

We thank the DFG for financial support and the ''Vigoni'' program for traveling funds. One of us (N.V.D.) wishes to thank the staff of the Heidelberg University Theoretical Chemistry Department for hospitality and the stimulating atmosphere. We express our gratitude to J. Schirmer and H. Köppel for stimulating discussions.

*Permanent address: Institute of Automation & Control Processes, 690041, Vladivostok, Russia.

[1] J. C. Fuggle, T. E. Madey, M. Steinkilberg, and D. Menzel, Chem. Phys. Lett. **33**, 233 (1975).
[2] J. C. Fuggle, E. Umbach, D. Menzel, K. Wandelt, and C. R. Brundle, Solid State Commun. **27**, 65 (1978).
[3] P. R. Norton, R. L. Tapping, and J. W. Goodale, Surf. Sci. **72**, 33 (1978).
[4] C. R. Brundle, P. S. Bagus, D. Menzel, and K. Hermann, Phys. Rev. B **24**, 7041 (1981).
[5] E. Umbach, Surf. Sci. **117**, 482 (1982).
[6] N. Mårtensson and A. Nilsson, J. Electron Spectrosc. Relat. Phenom. **52**, 1 (1990).
[7] H. Tillborg, A. Nilsson, and N. Mårtensson, J. Electron Spectrosc. Relat. Phenom. **62**, 73 (1993).
[8] K. Schönhammer and O. Gunnarsson, Solid State Commun. **23**, 691 (1977); K. Schönhammer and O. Gunnarsson, Z. Phys. B **30**, 297 (1978).
[9] N. D. Lang and A. R. Williams, Phys. Rev. B **16**, 2408 (1977).
[10] D. A. Shirley, Chem. Phys. Lett. **16**, 220 (1972).
[11] B. Gumhalter and D. M. Newns, Phys. Lett. A **57**, 423 (1976).
[12] B. Gumhalter, J. Phys. C **10**, L219 (1977).
[13] B. Gumhalter, K. Wandelt, and Ph. Avouris, Phys. Rev. B **37**, 8048 (1988).
[14] O. Gunnarsson and K. Schönhammer, Solid State Commun. **26**, 147 (1978).
[15] O. Gunnarsson and K. Schönhammer, Phys. Scr. **21**, 575 (1980).
[16] B. Gumhalter, Prog. Surf. Sci. **15**, 1 (1984).
[17] D. Lovrić, B. Gumhalter, and K. Wandelt, Surf. Sci. **278**, 1 (1992).
[18] H.-J. Freund, H. Pulm, B. Dick, and R. Lange, Chem. Phys. **81**, 99 (1983).
[19] C. M. Kao and R. P. Messmer, Phys. Rev. B **31**, 4835 (1985).
[20] H.-J. Freund, R. P. Messmer, C. M. Kao, and E. W. Plummer, Phys. Rev. B **31**, 4848 (1985).
[21] N. V. Dobrodey, L. S. Cederbaum, and F. Tarantelli, Phys. Rev. B **54**, 10 405 (1996).
[22] R. P. Messmer, S. H. Lamson, and D. R. Salahub, Solid State Commun. **36**, 265 (1980); Phys. Rev. B **25**, 3576 (1982).
[23] M. Ohno and P. Decleva, Chem. Phys. **171**, 9 (1993).
[24] A. Nilsson, N. Mårtensson, S. Svensson, L. Karlsson, D. Nordfors, U. Gelius, and H. Ågren, J. Chem. Phys. **96**, 8770 (1992).
[25] E. Umbach, Solid State Commun. **51**, 365 (1984).
[26] W. F. Egelhoff, Jr., Surf. Sci. **141**, L324 (1984).
[27] A. Nilsson, H. Tillborg, and N. Mårtensson, Phys. Rev. Lett. **67**, 1015 (1991).
[28] M. Ohno and P. Decleva, Surf. Sci. **269/270**, 264 (1992).
[29] M. Ohno and P. Decleva, Chem. Phys. **160**, 341 (1992).
[30] S. Kono, S. M. Goldberg, N. F. T. Hall, and C. S. Fadley, Phys. Rev. B **22**, 6085 (1980).
[31] J. Schirmer, L. S. Cederbaum, and O. Walter, Phys. Rev. A **28**, 1237 (1983).
[32] G. Angonoa, O. Walter, and J. Schirmer, J. Chem. Phys. **87**, 6789 (1987).
[33] M. W. Schmidt *et al.*, QCPE Bull. **10**, 52 (1990).
[34] M. F. Guest and P. Sherwood, *Gamess-UK User's Guide and Reference Manual* (Daresbury Laboratory, Daresbury, 1992).
[35] C. W. Bauschlicher, Jr., Chem. Phys. Lett. **115**, 387 (1985).
[36] B. Roos, A. Veillard, and G. Vinot, Theor. Chim. Acta **20**, 1 (1971).
[37] A. J. H. Wachters, J. Chem. Phys. **52**, 1033 (1970).
[38] P. J. Hay, J. Chem. Phys. **66**, 4377 (1977).
[39] *Gaussian Basis Sets for Molecular Calculations*, edited by S.

Huzinaga, Physical Sciences Data Vol. 16 (Elsevier, Amsterdam, 1984).
[40] W. Domcke and L. S. Cederbaum, Chem. Phys. **25**, 189 (1977).
[41] L. S. Cederbaum, J. Schirmer, and H.-D. Meyer, J. Phys. A **22**, 2427 (1989).
[42] L. S. Cederbaum, W. Domcke, J. Schirmer, and W. von Niessen, Adv. Chem. Phys. **65**, 115 (1986).
[43] N. V. Dobrodey, L. S. Cederbaum, and F. Tarantelli (unpublished).
[44] W. Domcke, L. S. Cederbaum, J. Shirmer, and W. von Niessen, Phys. Rev. Lett. **42**, 1237 (1979).
[45] L. S. Cederbaum, W. Domcke, and J. Schirmer, Phys. Rev. A **22**, 206 (1980).
[46] A. Barth and J. Schirmer, J. Phys. B **18**, 867 (1985).
[47] M. Fink and A. C. Yates, At. Data **1**, 385 (1970); K. Zähringer,H.-D. Meyer, and L. S. Cederbaum, Phys. Rev. A **46**, 5643 (1992).
[48] In the frozen-orbital approximation the orbitals of the ground state are used to compute the energies of the ionized states as single-configuration expectation values of the total Hamiltonian.
[49] C. W. Bauschlicher, Jr., S. R. Langhoff, and L. A. Barnes, Chem. Phys. **129**, 431 (1989); M. R. A. Blomberg, U. Brandemark, P. E. M. Siegbahn, K. Broch-Mathisen, and G. Karlströom, J. Phys. Chem. **89**, 2171 (1985); C. W. Bauschlicher, Jr., P. S. Bagus, C. J. Nelin, and B. O. Roos, J. Chem. Phys. **85**, 354 (1986).
[50] M. Ohno and P. Decleva, Surf. Sci. **258**, 91 (1991); Chem. Phys. **156**, 309 (1991).
[51] M. Ohno, J. Electron Spectrosc. Relat. Phenom. **69**, 225 (1994).